scientific reports

Check for updates

OPEN

Impaired degree centrality and effective connectivity contributed to deficits in cognition and depression in patients with temporal lobe epilepsy

Bailing Qin, Shujun Su, Xuemei Chen, Yuting Sun, Qin Zhou, Huoyou Hu, Lu Qin & Jinou Zheng✉

Temporal lobe epilepsy (TLE) leads to severe neuropsychiatric symptoms and cognitive impairment; however, the underlying mechanism is still not fully understood. Using degree centrality (DC), effective connectivity (EC), and multivariate pattern analysis (MVPA), we aimed to reveal alterations in brain networks and investigate neurofunctional symptoms in TLE patients. A total of fifty TLE patients and forty-seven healthy controls (HCs) were enrolled and underwent resting-state functional magnetic resonance imaging (rsfMRI) and neuropsychological testing. Cerebral functional activity and neuroimaging features were differentiated between the patient and HC groups based on rsfMRI data, DC, EC, and MVPA. Patients showed signs of depression, anxiety, and cognitive impairments in comparison to HCs. DC analysis revealed that patients had greater DC in the right inferior temporal gyrus and lower DC in the left and right cuneus than the HCs did. EC analysis revealed decreased EC from the right cuneus, right praecuneus, right superior occipital gyrus and right lingual gyrus to the left cuneus and increased EC from the left cuneus to the left calcarine sulcus and left middle occipital gyrus in TLE patients compared with HCs. The MoCA and Hamilton Depression Scale scores were correlated with impaired cerebral functional connectivity, according to correlation analysis. The MVPA classifier yielded an area under the curve of 0.91, an accuracy classification rate of 82.47%, a sensitivity of 85.11%, and a specificity of 80.00% according to the granger causality analysis(GCA) maps and receiver operating characteristic curve analysis. According to the current study, patients with TLE may have cognitive and depressive deficits as a result of abnormalities in the hub and related nodes in the default mode network and visual network. Moreover, the GCA might be a good imaging feature for the diagnosis of TLE.

Keywords Temporal lobe epilepsy, Degree centrality, Granger causality analysis, Multivariate pattern analysis

Temporal lobe epilepsy (TLE) is the most common type of focal epilepsy and is often associated with cognitive and emotional disorders[1]. The pathogenesis of cognitive and emotional disorders in patients with TLE is still unclear, and whether they are related to changes in brain networks has not been fully elucidated.Traditionally, localized structural damage to the hippocampal and temporal lobes is common in TLE patients. However, functional magnetic resonance imaging (fMRI) data indicate that seizures can impact brain networks on a large scale, starting in the temporal lobe and spreading to other regions of the brain[2].

Functional connectivity (FC) has been extensively utilized in the study of epilepsy[3]. Shi et al. reported that brain regions with altered voxel-mirrored homotopic connectivity had abnormal directed FC with multiple brain regions, mainly those belonging to the default mode network, sensorimotor network, and visual network[4]. In accordance with the broad seizure onset and propagation pathway, Dumlu et al. reported that TLE patients exhibited increased variability, primarily in the frontoparietal control, default mode, dorsal/ventral attention, visual, and somatomotor networks[5]. These networks are linked to functional deficits in executive functioning,

Department of Neurology, The First Affiliated Hospital of Guangxi Medical University, Nanning, China. ✉email: jinouzheng@163.com

memory, and attention. Gao et al. reported that patients with left TLE have decreased network homogeneity in the right inferior temporal gyrus and the left middle temporal lobe and increased network homogeneity in the bilateral praecuneus and right inferior parietal lobe[6]. These findings support the theory that the functional disruption caused by TLE extends beyond the temporal lobe and into other regions of the cortex. Additionally, a complex network of alterations may mediate epilepsy, and aberrations in the default network, visual network microstructure, and FC may constitute significant characteristics of TLE.

Few studies have investigated changes in topological properties, and most traditional FC studies have concentrated on the FC of seed points or independent component analysis[7]. Without the need to choose a region of interest (ROI), voxel-level graph analysis of degree centrality (DC) can represent the network centre's nodes for quantitative analysis. By identifying the direct association of each node with every other node in the brain, DC can be used to assess the relative importance of each node within the brain network at the global network level. Thus, DC represents the hub distribution across functional brain networks as well as information processing and communication capabilities[8].

The quantity of FC values can partially compensate for the limitations of conventional FC research by reflecting the intricate characteristics of brain network traffic. This method has been extensively utilized to study how diseases impact specific aspects of the brain network[9]. Effective connectivity (EC) measures neural activity as a causal effect of one region on another, whereas FC only measures instantaneous temporal correlations between spatially different brain regions. Consequently, an EC analysis may offer a more thorough explanation of the neuropathology of TLE by describing the information flow between different brain regions[10]. Granger causality analysis (GCA) has been used recently to examine EC in brain networks associated with epilepsy. Using GCA, Jiang et al. discovered that patients with refractory epilepsy had altered EC in the dorsal attention network, ventral attention network, and default mode network (DMN), which affected how information was communicated between networks[11]. Ke et al. used the sliding window technique in conjunction with GCA to treat patients with juvenile myoclonic epilepsy; this method identified notable disturbances in the local characteristics of the whole-brain functional connectivity network, which indicated causal impairments across several functional networks[12].

Epilepsy is believed to be caused by a disruption of functional networks[13]and a growing body of research indicates that interactions between several networks play a significant role in the onset of TLE[14]. Both DC and GCA can characterize the functional connectivity of the brain. When the regions of interest (ROIs) are not initially defined. DC can be used to evaluate the importance of each node in the brain network by determining its direct association with the remaining nodes in the whole brain at the global network level. By defining hubs as ROIs in subsequent analyses via the GCA approach, networks between the hub and other brain regions that are disrupted can be further displayed at the global level to reveal pathogenetic mechanisms from different perspectives. To the best of our knowledge, this combined analysis has not yet been performed in patients with TLE. For a more thorough investigation of aberrant brain functional connectivity in TLE patients, DC and EC were combined in the current study.

In this study, abnormal cerebral functional activity and connectivity, as well as how they may impact neuropsychological impairments, in TLE patients were investigated. We identified brain regions with DC values that differed between TLE patients and healthy controls (HCs) to characterize important nodes and networks in TLE patients. We subsequently used EC to determine the direction of these connection changes. Additionally, correlation analysis was carried out to determine how cognitive and emotional impairments in patients with TLE are impacted by abnormal functional activity and the associated networks of cerebral hubs.

Resting-state fMRI studies have focused mainly on group-level differences according to univariate analysis, ignoring information about spatial distribution patterns. Multivariate pattern analysis (MVPA) is a machine learning-based approach that can be used with rs-fMRI data to detect promising biomarkers and is sensitive to spatially distributed information. MVPA overcomes the limitations of rigid multiple comparison correction and the low signal-to-noise ratio of a single voxel by analysing the interactions between multiple voxels[15]. However, whether DC and GCA can be used to distinguish between TLE patients and healthy controls needs further clarification through MVPA.

In conclusion, the aims of our study were to reveal the functional connectivity of the brain using DC and GCA and to uncover the underlying mechanisms of cognitive decline and psychiatric disorders in TLE patients.

Materials and methods

Participants

Fifty right-handed TLE patients who met the diagnostic criteria of the International League Against Epilepsy (2017) were included in the study[16]. The inclusion criteria were as follows: (a) the patient's clinical manifestations were consistent with the semiology of TLE; (b) the patient's clinical data were complete, and the frequency of episodes was more than twice a year; (c) the patient exhibited complex partial seizures with amnesia or decreased responsiveness to vocal instructions or questions; (d) the patient was between the ages of 18 and 55; and (e) the patient was receiving antiseizure medication, which had not changed in the last three months. The exclusion criteria included a history of substance abuse, prior neurological conditions, and MRI contraindications. In total, 47 healthy right-handed participants who matched the TLE group in terms of age, sex, and educational attainment were selected. All right-handed participants finished the entire experiment. The Hamilton Anxiety Scale (HAMA) and Hamilton Depression Scale (HAMD24) were used to measure anxiety and depression[17]respectively, and the Montreal Cognitive Assessment (MoCA) was used to assess cognitive function[18]. This study protocol was approved by the Ethics Committee of the First Affiliated Hospital of Guangxi Medical University, and informed consent was obtained from all participants. All the experiments were performed in accordance with the relevant guidelines and regulations.

Magnetic resonance imaging acquisition and data preprocessing

We performed rsfMRI scans at Guangxi Medical University's First Affiliated Hospital. A Phillips Medical Systems Nederland B.V. Achieva 3T scanner was used to collect the MRI data. A gradient-echo planar picture sequence was performed with the following parameters: repetition time: 2,000 ms; echo time: 30 ms; flip angle: 90°; field of view: 220 × 220 mm; voxel size: 3.44 × 3.44 × 3.50 mm; matrix size: 64 × 64; slice number: 41; slice gap: 0.5 mm; and value number: 225 slices.

All the participants were asked to remain awake, keep their eyes closed, and maintain a relaxed, quiet state throughout the scanning procedure. Spongy pads were used to stabilize the head, and headphones were used to reduce the effects of noise. The scanning process took approximately eight minutes in total.

The fMRI data were preprocessed via RESTplus_v1.28 software (Forum of resting-state fMRI (restfmri.net))[19]. For every subject, the first ten fMRI pictures were deleted. Subsequently, realignment was performed to check head motion, and slice timing was used to correct time differences. The subject was eliminated from the study if the average head movement exceeded 3.0 mm or if the head rotation angle exceeded 3°. Coregistration between the functional images and T1-weighted images was performed for all subjects. All T1-weighted images were then segmented. The diffeomorphic anatomical registration through exponentiated Lie algebra (DARTEL) template was used to create a sample-specific diffeomorphic anatomical registration using the structural images of each subject[20]. Using the DARTEL template and the matching flow field, the functional images were normalized to the Montreal Neurological Institute (MNI) space before being resampled to 3 mm×3 mm×3 mm. Next, detrending and filtering (bandpass, 0.01–0.08 Hz) were applied to the data. White matter and cerebrospinal fluid signals were regressed.

Degree centrality analysis

RESTplus_v1.28 software was used for DC analysis, and the voxel-based whole-brain DC was calculated. In brief, each voxel is regarded as a node, and the edges are represented by the Pearson correlation—a linear correlation between voxels that indicates neural activity. In the brain template, the correlations between any two voxels were computed for every subject, and domain values ($r > 0.25$) were then established for each set of correlations. The DC of each individual level was determined, and the entire brain functional network was built using each correlation threshold, which was set at $r > 0.25$. Finally, by dividing by the average DC value of the entire brain, the standardized DC value was found. The correlation coefficients were transformed to Z values using the Fisher Z transform to improve the normality of the data. Subsequent statistical analysis was performed after the DC plots were smoothed using a 6-mm FWHM Gaussian smoothing kernel. A single node's significance in the brain was represented by DC, which also symbolized the "hub" quality of the functional network[21].

Effective connectivity analysis

To assess the impact of directionality, we utilized GCA to assess EC changes. We chose regions of interest from among the brain regions that revealed notable differences between TLE patients and HCs according to the DC analysis. All ROI coordinates were in MNI space. GCA was performed with RESTplus_v1.28 software[22]. Abnormal brain regions with increased or decreased strength in the DC analysis were employed as seed points for GCA; the whole brain was considered time series Y, and the seed points were considered time series X. By determining the influence of X on Y and the influence of Y on X, Granger causality maps were produced. These Granger causality maps were used as the basis for the Fisher z-transformation, which produced the Z score. After the causal coefficient matrix was built, the coefficient showed the direction and degree of functional connectivity[23].

Multivariate pattern analysis

We used PRONTO Software version 2.0 on the MATLAB2022 platform (https://www.mathworks.cn) to perform MVPA of the GCA signals of the two groups of participants[24]. We established classification models for the TLE and HC groups using binary support vector machines. To determine the statistical significance of the voxel changes in the brain regions, 1000 permutation tests were conducted. Finally, the diagnostic value of GCA maps in distinguishing between patients and healthy controls was analysed through classification maps, subject working characteristic curves, and weight maps of each brain region.

Statistical analysis and correlation analysis

Statistical analysis was conducted using SPSS 27.0 software. The results are displayed as a number or mean ± standard deviation. Age, education level, MoCA score, HAMA score, and HAMD24 score were compared between the groups using two independent sample t tests. Sex comparisons were conducted via the $\chi 2$ test. To assess the correlation between the Pearson or Spearman values and clinical features, the functional activity intensity of key brain regions was extracted from the DC analysis and GCA. The difference was statistically significant at $P < 0.05$[25]. Gaussian random field correction ($p < 0.05$) or false discovery rate correction ($p < 0.01$) was used to correct the results and identify the activated brain regions.

Results

Demographic information and clinical features

Fifty patients with TLE and forty-seven matched healthy controls were recruited for this study. Age, sex, and education did not differ between the TLE and HC groups. In terms of neuropsychological assessments, MoCA scores were lower in the TLE group than in the HC group. The HAMA and HAMD24 scores were greater in the TLE group than in the HC group. All demographic, clinical and neuropsychological data are listed in Table 1.

Characteristic	TLE($n=50$)	HC($n=47$)	Statistical value	p Value
Sex (male/female)	16/34	23/14	2.979[b]	0.084
Age (years)	30.48(15,49)	29.60(21,54)	-0.336[a]	0.336
Education (years)	12.06(3,16)	13.38(3,18)	-1.331[a]	0.183
Handedness (right/left)	25/25	NA	NA	NA
Duration (years)	7(9)	NA	NA	NA
MoCA, score	27 ± 4	29 ± 2	-4.418[a]	<0.001*
HAMD24,score	4 ± 7	1 ± 3	-4.989[a]	<0.001*
HAMA, score	3 ± 5	0 ± 1	-5.564[a]	<0.001*

Table 1. Demographic, clinical and neuropsychological features for patients with TLE and HC. *TLE* temporal lobe epilepsy, *HC* healthy control, *MoCA* the montreal cognitive assessment, *HAMD24* Hamilton depression scale; *HAMA* Hamilton anxiety scale. [a] p Value was calculated by a Mann–Whitney U-test. [b] p Value was calculated by the chi-square test. * The results were statistically signifcant ($P<0.05$).

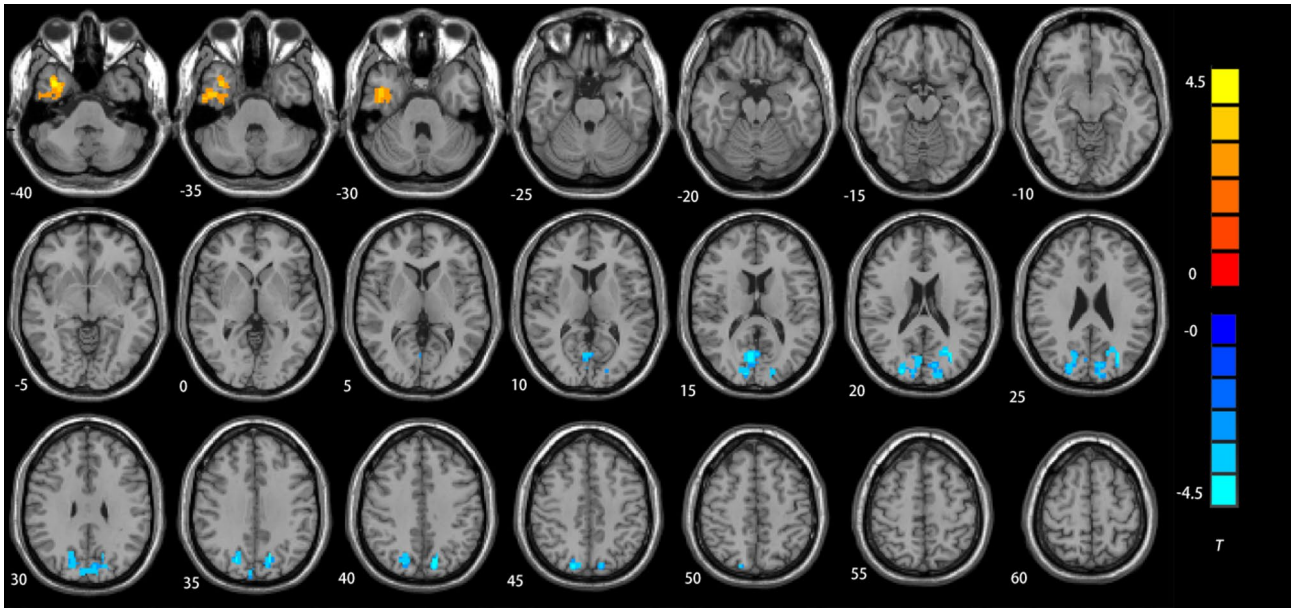

Fig. 1. Alterations in DC strength in patients with TLE. The altered brain regions were located in the right inferior temporal gyrus、 right cuneus and left cuneus. Gaussian random field correction was set at voxellevel $P<0.005$ and clusterlevel $P<0.05$. The color bar with Tvalues indicates the strength of functional activity (a warm color represents increased functional strength, while a cool color represents decreased functional strength).

Brain regions	Abbreviation	MNI coordinate			Cluster size	t-value
		X	Y	Z		
Inferior temporal gyrus_R	ITG.R	36	3	-42	183	5.4263
Cuneus_R	CUN.R	9	-75	18	281	-4.4401
Cuneus_L	CUN.L	-12	-78	42	230	-4.5719

Table 2. Comparison of the DC values between TLE patients and HC. *MNI* Montreal neurological institute, *R* right,*L* left, *GRF* correction, voxel-level: $p<0.005$ and cluster-level: $p<0.05$.

Degree centrality analysis

Figure 1 illustrates the distinctions between the patient group and the HC group according to the DC analysis results, while Table 2 displays the DC values of various brain regions (GRF correction, voxel-level: $p<0.005$ and cluster-level: $p<0.05$). As shown in Fig. 1; Table 2, the DC intensity of the right inferior temporal gyrus (ITG.R)

was greater in TLE patients than in HCs. In addition, the DC intensity of the right cuneus (CUN.R) and left cuneus (CUN.L) was lower in the patient group than in the HC group.

Effective connectivity analysis

Brain regions with statistically significant differences in DC strength were selected as ROIs for GCA. In the analysis of effective connectivity from the CUN.L to the whole brain, patients with TLE had an increased intensity of connection to the left calcarine (CAL.L) and left middle occipital gyrus (MOG.L) surrounding the cortex compared with the HC group (FDR correction; $P < 0.01$; Fig. 2; Table 3). Connectivity from the CUN.R, right praecuneus (PCUN.R), right superior occipital gyrus (SOG.R) and right lingual gyrus (LING.R) to the CUN.L was decreased in the TLE group (FDR correction; $P < 0.01$; Fig. 3; Table 3). At the whole-brain level, no significant differences in the other brain ROIs from the automated anatomical labelling atlas between the patient group and the HC group were observed.

Correlation results

Further analysis was conducted on the correlations between clinical characteristics and functional activity in the brain regions that showed significant differences in DC analysis and GCA. The DC strength in the right inferior

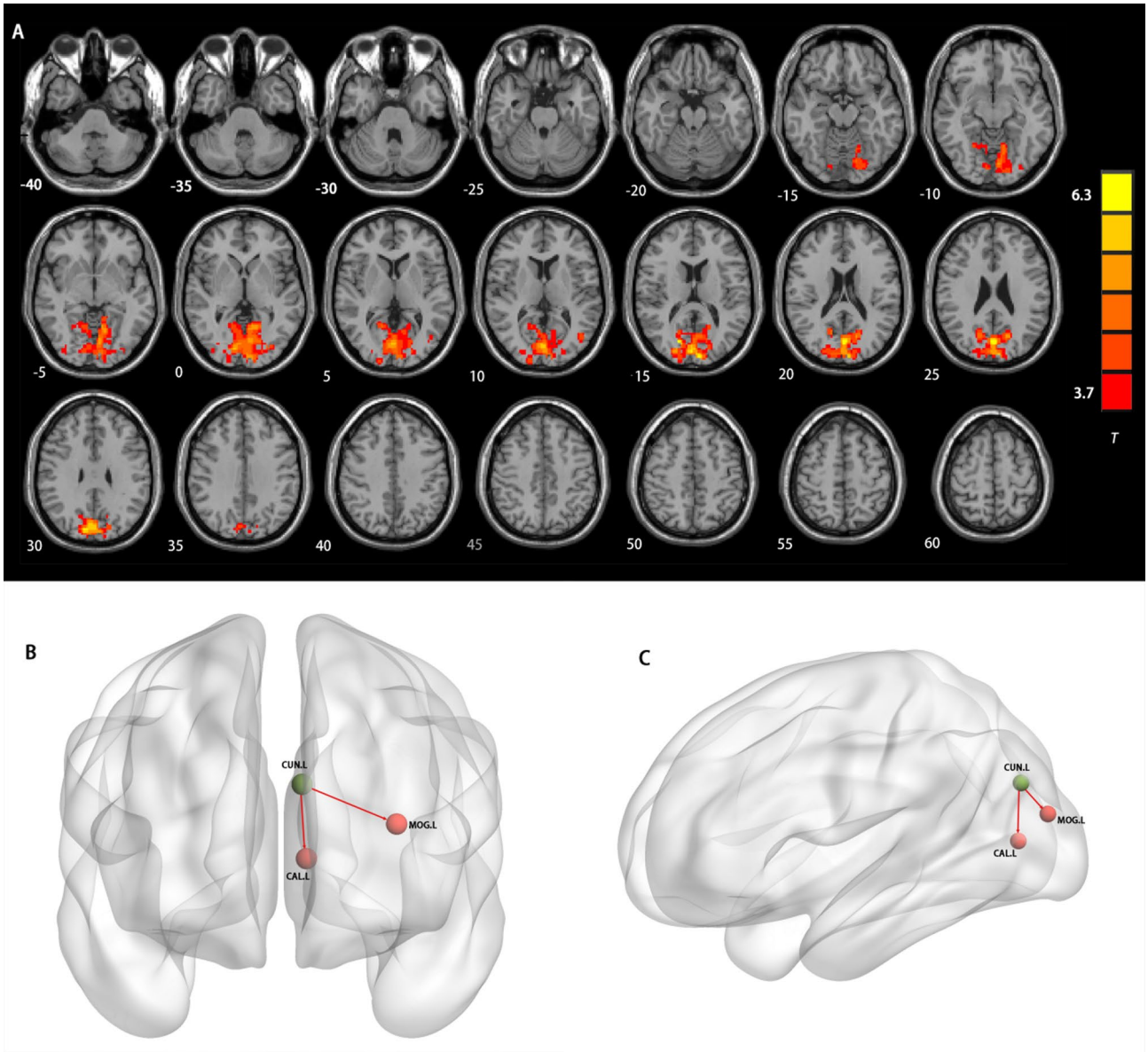

Fig. 2. Between-group diferences in GCA. The warm color represents increased effective connectivity. The cool color represents decreased effective connectivity. The arrow represents the direction of the functional connectivity. The green color represents the seed point. (**A**,**B**,**C**): The effective connectivity from the left cuneus to other brain regions. Figure (**B**) and (**C**) wre generated using the BrainNet Viewer toolbox.*CUN.L* left cuneus, *CAL.L* left calcarine, *MOG.L* left middle occipital gyrus.

Brain regions	Abbreviation	MNI coordinate			Cluster size	t-value
		X	Y	Z		
Cuneus_L to the whole brain						
Calcarine_L	CAL.L	0	-78	27	1826	6.8654
Middle occipital gyrus_L	MOG.L	-45	-69	9	18	4.6962
The whole brain to Cuneus_L						
Cuneus_R	CUN.R	3	-75	27	527	-6.725
Precuneus_R	PCUN.R	15	-63	21	33	-5.6362
Superior occipital gyrus_R	SOG.R	24	-87	15	17	-5.0363
Lingual gyrus_R	LING.R	18	-84	0	17	-5.1232

Table 3. Comparison of the GCA values between TLE patients and HC. *MNI* montreal neurological institute; *R* right,*L* left, FDR correction, voxel-level: $p < 0.01$.

temporal gyrus was negatively correlated with the MoCA score (r=-0.329; $P = 0.022$; Fig. 4A). According to GCA, HAMD24 scores were negatively correlated with connectivity from the right cuneus to the left cuneus (r=-0.283; $P = 0.047$; Fig. 4B).

Multivariate pattern analysis

In the present study, specific effective connectivity in patients with TLE compared with HCs was identified by using MVPA to analyse neural signals on the basis of GCA maps. The AUC of the ROC curve was 0.91 for the connectivity from the CUN.L to the CAL.L and 0.84 for the connectivity from the CUN.R to CUN.L (Table 4). The classification accuracy was 82.47%, and the sensitivity and specificity were 85.11 and 80.00%, respectively. MVPA based on GCA from CUN.L to CAL.L exhibited good performance in differentiating the TLE group from the HC group (Fig. 5). The primary associated brain regions included the left cuneus, left calcarine fissure and surrounding cortex and left middle occipital gyrus between the two groups. This analysis suggested that MVPA classifiers can be used to differentiate between HCs and TLE patients.

Discussion

According to recent studies on brain networks, diseases linked to modifications in brain network function usually impact a few key core nodes rather than the entire brain[26,27]. The central nodes involved in information processing in the brain network are crucial components[28]. A number of alterations in functional networks may result from lesion-induced modifications in the functionality of the core nodes[26]. DC is typically indicative of the core nodes of the network, whereas EC can show anomalies in directional connectivity in key brain regions[29].

Through DC analysis, we discovered abnormal DC values within the ITG.R, CUN.R and CUN.L in patients with TLE in this study. We subsequently used the regions with differences in DC as seed regions for analysis of the EC of the whole brain via the GCA algorithm. The TLE patients presented increased EC from the CUN.L to the whole brain, including from the CUN.L to the CAL.L and from the CUN.L to the MOG.L and decreased connectivity from the CUN.R, PCUN.R, SOG.R and LING.R to the CUN.L. Additionally, the DC strength in the ITG.R was negatively correlated with the MoCA score, and the EC from the CUN.R to the CUN.L was negatively correlated with HAMD24 score. Moreover, patients with TLE could be distinguished from HCs with high accuracy and sensitivity by using disrupted GCA maps and MVPA. In conclusion, the current study identified the characteristics of impaired functional hubs and their associated networks in TLE patients, offering a more thorough understanding of the process behind pathological damage in this illness.

In this study, we observed increased DC in the ITG.R. The ITG is well known to play a role in higher-order cognitive processes, such as emotion regulation and language and visual comprehension[30]. The ITG is connected to the frontal, parietal and marginal lobes by U-shaped fibres and longitudinal, bow and uncinate tracts[30]. Consequently, the ITG is an important part of the global brain network, and abnormal ITG activation may affect temporal lobe function[31]. Shi et al. reported a correlation between temporal lobe epilepsy and alterations in functional homotopy and connectivity in the ITG[4]. It has also been reported that major depressive disorder is linked to ITG activation[32]. Our study demonstrated that increased DC in the ITG.R was negatively correlated with the MoCA score, indicating a decline in cognitive function, which is essentially consistent with other reports[33]. Thus, as previously noted, abnormalities in the ITG may serve as a neuroimaging marker for brain disorder diagnosis and prognosis[34]. In conclusion, the regions of the ITG.R that showed increased DC in this study may be indicative of a compensatory mechanism to maintain cognitive needs in the brains of TLE patients[35]. These findings also imply that the region is more significantly important and plays a more central role than it typically does and that it has stronger functional connectivity with other areas of the brain. Another theory is that the neuronal hyperactivity of this region could lessen or offset structural brain damage.

Decreased DC values in TLE patients were mainly observed in the CUN.R and CUN.L. An fMRI study revealed significant repetition enhancement in the right cuneus and supported a specific role for the cuneus in spatial frequency processing[36]. Wang et al. reported that decreased grey matter volume in the cuneus and increased cuneus-prefrontal negative functional connectivity may play important roles in poor treatment outcomes in alcoholics and may serve as imaging markers for predicting relapse[37]. He et al. suggested that left cuneus volume may be related to working memory[38]. Furthermore, Li et al. reported that patients with

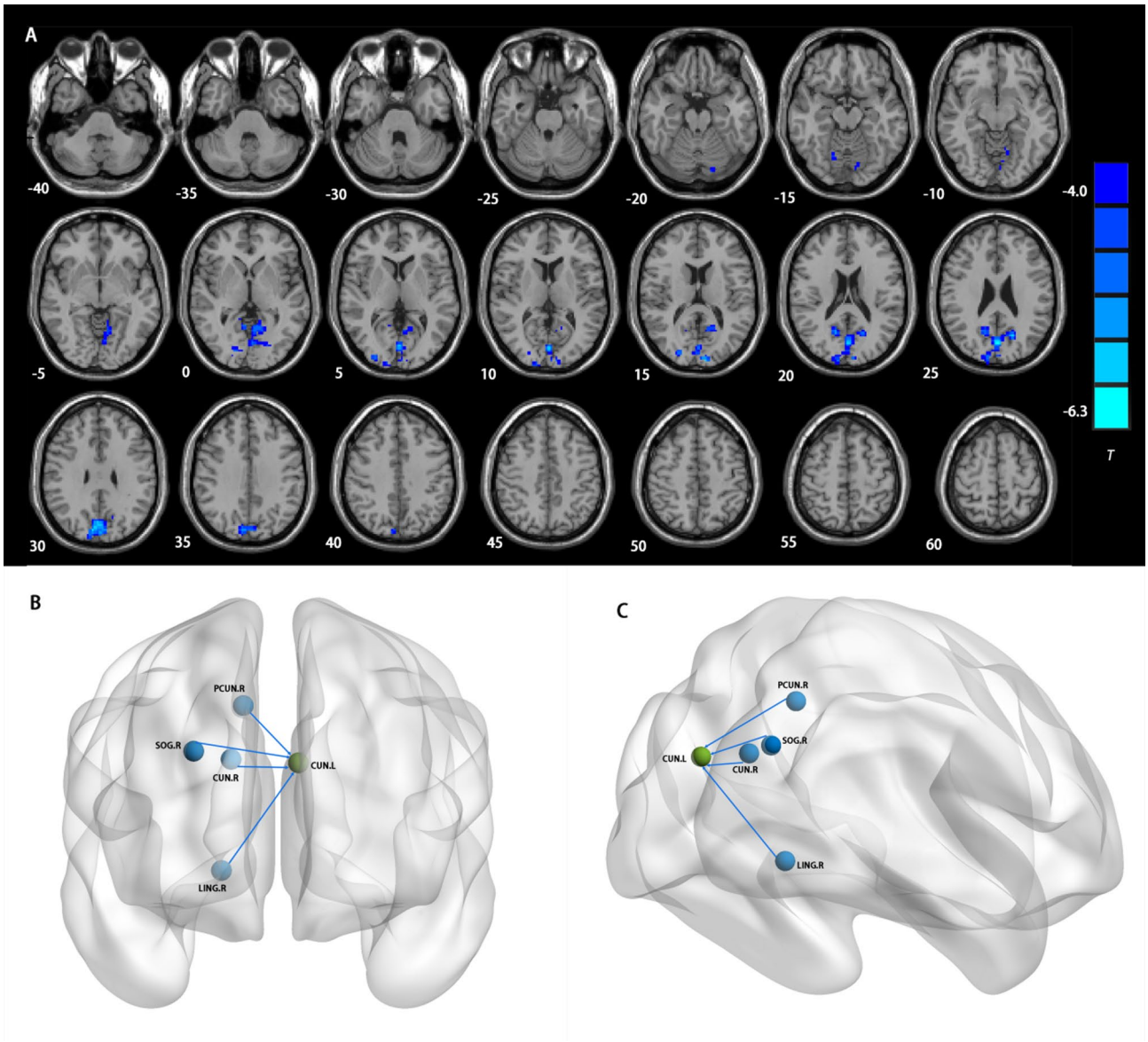

Fig. 3. Between-group diferences in GCA. The warm color represents increased effective connectivity. The cool color represents decreased effective connectivity. The arrow represents the direction of the functional connectivity. The green color represents the seed point. (**A**,**B**,**C**): The effective connectivity from other brain regions to left cuneus. Figure B and C wre generated using the BrainNet Viewer toolbox. *CUN.L* left cuneus, *CUN.R* right cuneus, *PCUN.R* right precuneus, *SOG.R* right superior occipital gyrus,*LING.R* right lingual gyrus.

persistent postural-perceptual dizziness exhibited altered spontaneous functional activity in the cuneus and praecuneus, which may result in abnormal integration of vestibular and visual information. When standing or moving, symptoms may worsen if the functional connectivity between the praecuneus and precentral gyrus is decreased[39]. The cuneus, a smaller lobe in the occipital lobe of the brain involved in basic visual processing, is a wedge-shaped area between the talar and medial parieto-occipital fissures[40]. The cuneus is also known to facilitate cross-modal, nonvisual functions, such as linguistic processing and verbal memory, after the loss of visual senses. Therefore, in this study, the decreased DC values of the cuneus in TLE patients could be interpreted as impaired visual processing ability and impaired ability of these functional brain regions to facilitate neural network connections. Furthermore, impaired visual processing ability may indirectly impact a patient's alertness and cognitive functions[41]. Therefore, patients with TLE often present visual abnormalities and symptoms of cognitive impairment.

GCA based on seed points in brain regions with varying DC values was utilized in this study to examine the changes in EC among the core brain networks. Our results revealed increased EC from the left cuneus to the regions of the visual network (VN), including from the CUN.L to the CAL.L and from the CUN.L to the MOG.R. The CAL.L and MOG.R are the cortex of the visual centre and are necessary for both basic and higher-level

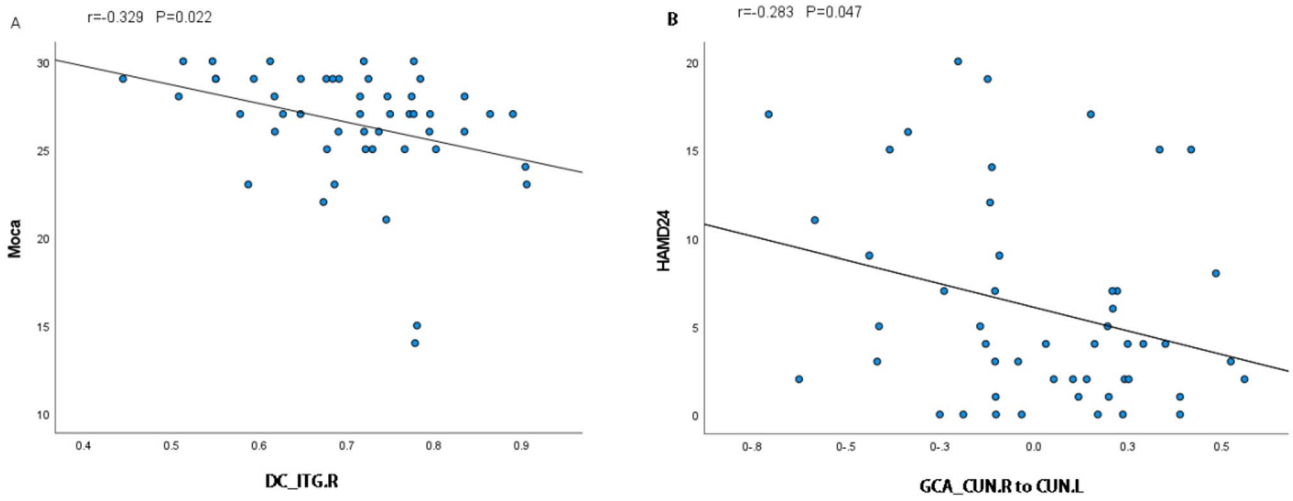

Fig. 4. Analysis of correlations between clinical parameters and functional activity features. (**A**) The DC strength of the right inferior temporal gyrus was negatively correlated with the MoCA score (r=-0.329; P = 0.022). (**B**) The effective connectivity from the right cuneus to the left cuneus was negatively correlated with the HAMD24 (r=-0.283; P = 0.047). *DC* degree centrality, *HAMD24* Hamilton depression scale.DC_ITG.R, DC values of right inferior temporal gyrus; GCA_CUN.R to CUN.L, the GCA values of right cuneus to the left cuneus.

Brain regions	AUC	Total accuracy (%)	Sensitivity (%)	Specificity (%)
CUN.L to CAL.L	0.91	82.47	85.11	80.00
CUN.R to CUN.L	0.84	80.41	76.60	84

Table 4. The ROC curves showing the ability of the GCA values to distinguish differences between the TLE and HC. *ROC* receiver operating characteristic curve, *AUC* area under the curve, *CUN.L* left cuneus, *CAL.L* left calcarine fissure and surrounding cortex, *CUN.R* right cuneus.

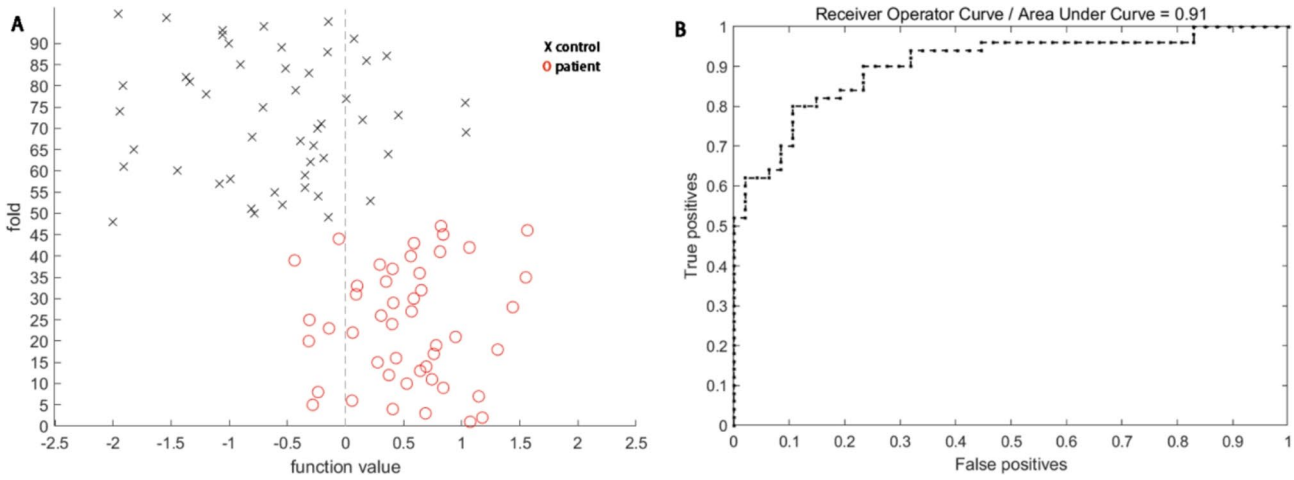

Fig. 5. Predictive value of the GCA. (**A**) Voxelbased predictive pattern. The GCA was able to distinguish between TLE patients and HC subjects. (**B**) Regionbased pattern localization map computed from the voxelbased predictive pattern. Receiver operating characteristic curve of the TLE patientsHC group classification model based on GCA maps with an accuracy of 82.47% (sensitivity, 85.11%; specificity, 80.00%). *GCA* Granger causality analysis, *TLE* temporal lobe epilepsy, *HC* healthy control.

visual processing. According to this study, the brain's possible adaptation mechanism to better execute pertinent visual tasks following cognitive function impairment in TLE patients could be explained by the increased EC of the CUN.L to the CAL.L and MOG.R in these patients.

The medial occipital lobe consists of the lingual gyrus and cuneus. Numerous studies have indicated that the cuneus participates in fundamental visual processing activities, such as those concerning motion, direction, speed, spatial frequency, and orientation[42]. Previous research has demonstrated that the lingual gyrus, which is involved in motion and direction discrimination, is activated preferentially when words are presented in lower contrast. Moreover, emotion and visual memory have been linked to the lingual gyrus. Selective visual amnesia can result from injury to the occipital lobe. According to research, flight training may increase the grey matter volume in the lingual gyrus; to avoid potential consequences, pilots must pay close attention to the instrumentation in the cockpit and thoroughly interpret any readings. The study also revealed an association between the lingual gyrus and the storage of visual memories[43]. In our study, the decreased EC of CUN.R, LING.R and SOG.R to CUN.L could be interpreted as the impaired ability of visual processing and visual memory in TLE patients.

As a vital node of the DMN, the praecuneus shows the highest activity when the human brain is in a healthy resting state[44]. The praecuneus is primarily involved in episodic memory, but it is also important for self-awareness, default mode processing, etc[45]. The praecuneus has four major types of anatomic connections: the superior parietal lobule, occipital cortex, frontal lobe, and temporal lobe. These connections offer another example of how higher-order information is integrated throughout the entire brain network[46]. TLE has been repeatedly shown to be linked to brain dysconnectivity in the DMN. Qin et al. reported that the praecuneus, cerebellum, and thalamus were the primary locations of blood oxygen level-dependent activation areas associated with high EEG network variation in TLE patients[47]. In contrast to HCs, some studies have demonstrated that patients with temporal lobe epilepsy exhibit aberrant EC between the praecuneus and the supramarginal gyrus[48]. Our results revealed decreased connectivity from the right praecuneus to the left cuneus in the TLE group. This finding is essentially consistent with previous research reports.

Data-driven analysis was utilized to examine the relationships between statistically significant brain regions and speculate about the possible structural configurations of neural connections through an efficient connectivity analysis. EC analysis has been employed in many recent studies on brain networks[49]. Harm to specific brain regions impacts not only how well those regions function normally but also the connections and pathways that allow information to flow between them. According to the results of this study, aberrant EC may underlie local pathway anomalies in TLE patients[50].

Correlation analyses were carried out in the current study between clinical features and the brain regions with significant differences in DC analysis and GCA. The MoCA score was negatively correlated with DC strength in the right inferior temporal gyrus. The HAMD24 score was negatively correlated with the GCA results from the right cuneus to the left cuneus. The temporal lobe is well known to be related to memory function. A more pronounced DC strength in the right inferior temporal gyrus in patients with TLE indicates more evident compensation and greater severity of primary damage, which will inevitably result in a decline in cognitive functions such as memory[51]. Marwood reported that cuneus activation can predict changes in certain clinical symptoms. A previous study demonstrated that abnormalities in the cuneus are related to depression[52]. Our study also revealed that decreased EC is associated with depressive symptoms. Taken together, the correlations found in this research reveal that abnormalities in the right inferior temporal gyrus and cuneus may be involved in the pathogenesis of deficits in cognition and emotion in patients with TLE.

MVPA can utilize spatial and temporal information from neuroimaging data as a potential diagnostic method for classifying people with many neurological and psychiatric diseases, such as autoimmune encephalitis, epilepsy, schizophrenia and depression[53]. Therefore, resting-state MRI may offer new evidence to support a TLE diagnosis, especially when the patient is still undergoing treatment or has not received a definitive diagnosis. In this study, by performing MVPA using GCA maps, we found that the AUC of the ROC curve was 0.91 for the CUN.L to the CAL.L, and the sensitivity and specificity of classification were high.

The brain regions identified by the DC analysis and GCA in the current investigation were consistent with each other. The aforementioned areas are linked to clinical symptoms in TLE patients, including psychiatric/behavioural abnormalities, cognitive impairment, and seizures. These regions are also involved in psychosis and cognitive function. In brief, GCA can help identify the imaging parameters that are implicated in the emergence of clinical symptoms. When paired with MVPA, GCA can be an effective diagnostic tool for TLE, particularly in patients who have nonspecific imaging findings or no abnormalities on routine MR images.

Limitations

Importantly, our study has several limitations. First, due to the lower temporal resolution of fMRI, TR limitations maybe affected the GCA results in short-term dynamic changes.In addition, bandpass filtering may lose important information in some signals.We did not apply the deconvolution method of the hemodynamic response function (HRF) to minimize the confounding effect of HRF.Second, our sample size was small. Further research should use large samples to enable subgroup analyses, considering the possible effects of seizure type, antiseizure medications, electroencephalograms, MR characteristics and other factors on functional connectivity. Third, because our study was cross-sectional in nature, it was challenging to draw conclusions about the causal relationships between the various brain functional network structures in TLE patients. To address this issue, we will improve our preprocessing methods in the future, and more longitudinal studies involving larger sample sizes are needed.

Conclusions

In summary, the current study showed that patients with TLE had disrupted DC and GCA results throughout the entire brain, with the DMN and VN being the primary locations. GCA was verified to be valid for building voxel-based analyses of seed points and whole-brain connectivity. These abnormal brain functional activities may be related to cognitive and depressive disorders and could provide imaging evidence for a deeper understanding of the pathological mechanisms of TLE. These findings also provide potential intervention targets for the treatment of cognitive and depressive disorders in TLE patients. For example, some neuroregulatory techniques such as transcranial magnetic stimulation or neurofeedback may target these brain regions or network to improve cognitive and depressive symptoms.Additionally, the primary diagnosis of TLE may be made with high accuracy, sensitivity, and specificity by combining GCA maps with MVPA and disrupted functional activity.

Data availability

The datasets generated and analyzed during the current study are available from the corresponding author on reasonable request.

Received: 22 August 2024; Accepted: 2 June 2025
Published online: 01 July 2025

References

1. Gao, Y. et al. Abnormal degree centrality as a potential imaging biomarker for right Temporal lobe epilepsy: A Resting-state functional magnetic resonance imaging study and support vector machine analysis. *Neuroscience* **487**, 198–206. https://doi.org/10.1016/j.neuroscience.2022.02.004 (2022).
2. Li, R. et al. Disruption of functional connectivity among subcortical arousal system and cortical networks in Temporal lobe epilepsy. *Brain Imaging Behav.* **14**, 762–771. https://doi.org/10.1007/s11682-018-0014-y (2019).
3. Li, W. et al. Altered resting state networks before and after Temporal lobe epilepsy surgery. *Brain Topogr.* **35**, 692–701. https://doi.org/10.1007/s10548-022-00912-1 (2022).
4. Shi, K. et al. Impaired interhemispheric synchrony and effective connectivity in right Temporal lobe epilepsy. *Neurol. Sci.* **45**, 2211–2221. https://doi.org/10.1007/s10072-023-07198-6 (2023).
5. Dumlu, S. N., Ademoğlu, A. & Sun, W. Investigation of functional variability and connectivity in Temporal lobe epilepsy: A resting state fMRI study. *Neurosci. Lett.* **733**, 135076. https://doi.org/10.1016/j.neulet.2020.135076 (2020).
6. Gao, Y. et al. Abnormal default-mode network homogeneity in patients with Temporal lobe epilepsy. *Medicine* **97** https://doi.org/10.1097/md.0000000000011239 (2018).
7. Ma, Y. & MacDonald Iii, A. W. Impact of independent component analysis dimensionality on the Test-Retest reliability of Resting-State functional connectivity. *Brain Connect.* **11**, 875–886. https://doi.org/10.1089/brain.2020.0970 (2021).
8. van den Heuvel, M. P. & Hulshoff Pol, H. E. Exploring the brain network: a review on resting-state fMRI functional connectivity. *Eur. Neuropsychopharmacol.* **20**, 519–534. https://doi.org/10.1016/j.euroneuro.2010.03.008 (2010).
9. Muccioli, L. et al. Cognitive and functional connectivity impairment in post-COVID-19 olfactory dysfunction. *Neuroimage Clin.* **38**, 103410. https://doi.org/10.1016/j.nicl.2023.103410 (2023).
10. Hua, M. et al. Disrupted pathways from limbic areas to thalamus in schizophrenia highlighted by whole-brain resting-state effective connectivity analysis. *Prog Neuropsychopharmacol. Biol. Psychiatry.* **99**, 109837. https://doi.org/10.1016/j.pnpbp.2019.109837 (2020).
11. Jiang, L. W. et al. Altered attention networks and DMN in refractory epilepsy: A resting-state functional and causal connectivity study. *Epilepsy Behav.* **88**, 81–86. https://doi.org/10.1016/j.yebeh.2018.06.045 (2018).
12. Ke, M., Hou, Y., Zhang, L. & Liu, G. Brain functional network changes in patients with juvenile myoclonic epilepsy: a study based on graph theory and Granger causality analysis. *Front. NeuroSci.* **18** https://doi.org/10.3389/fnins.2024.1363255 (2024).
13. Piper, R. J. et al. Towards network-guided neuromodulation for epilepsy. *Brain* **145**, 3347–3362. https://doi.org/10.1093/brain/awac234 (2022).
14. Hou, J. et al. Alterations in Cortical-Subcortical metabolism in Temporal lobe epilepsy with impaired awareness seizures. *Front. Aging Neurosci.* **14** https://doi.org/10.3389/fnagi.2022.849774 (2022).
15. Woo, C. W., Chang, L. J., Lindquist, M. A. & Wager, T. D. Building better biomarkers: brain models in translational neuroimaging. *Nat. Neurosci.* **20**, 365–377. https://doi.org/10.1038/nn.4478 (2017).
16. Scheffer, I. E. et al. ILAE classification of the epilepsies: position paper of the ILAE commission for classification and terminology. *Epilepsia* **58**, 512–521. https://doi.org/10.1111/epi.13709 (2017).
17. Tung, V. S. et al. Diagnostic value in screening severe depression of the Hamilton depression rating scale, Hamilton anxiety rating scale, Beck depression inventory scale, and zung's Self-Rating anxiety scale among patients with recurrent depression disorder. *Acta Inf. Med.* **31**, 249–253. https://doi.org/10.5455/aim.2023.31.249-253 (2023).
18. Jia, X. et al. A comparison of the Mini-Mental state examination (MMSE) with the Montreal cognitive assessment (MoCA) for mild cognitive impairment screening in Chinese middle-aged and older population: a cross-sectional study. *BMC Psychiatry.* **21**, 485. https://doi.org/10.1186/s12888-021-03495-6 (2021).
19. Jia, X. Z. et al. RESTplus: an improved toolkit for resting-state functional magnetic resonance imaging data processing. *Sci. Bull. (Beijing).* **64**, 953–954. https://doi.org/10.1016/j.scib.2019.05.008 (2019).
20. Ashburner, J. A fast diffeomorphic image registration algorithm. *Neuroimage* **38**, 95–113. https://doi.org/10.1016/j.neuroimage.2007.07.007 (2007).
21. Guo, R. et al. Abnormal hubs in global network as neuroimaging biomarker in right Temporal lobe epilepsy at rest. *Front. Psychiatry.* **13**, 981728. https://doi.org/10.3389/fpsyt.2022.981728 (2022).
22. Zang, Z. X., Yan, C. G., Dong, Z. Y., Huang, J. & Zang, Y. F. Granger causality analysis implementation on MATLAB: a graphic user interface toolkit for fMRI data processing. *J. Neurosci. Methods.* **203**, 418–426. https://doi.org/10.1016/j.jneumeth.2011.10.006 (2012).
23. Shi, Y. et al. Investigation of the emotional network in depression after stroke: A study of multivariate Granger causality analysis of fMRI data. *J. Affect. Disord.* **249**, 35–44. https://doi.org/10.1016/j.jad.2019.02.020 (2019).
24. Aglieri, V., Cagna, B., Velly, L., Takerkart, S. & Belin, P. FMRI-based identity classification accuracy in left Temporal and frontal regions predicts speaker recognition performance. *Sci. Rep.* **11**, 489. https://doi.org/10.1038/s41598-020-79922-7 (2021).
25. De La Pava Panche, I., Alvarez-Meza, A. M. & Orozco-Gutierrez, A. A Data-Driven measure of effective connectivity based on renyi's α-Entropy. *Front. Neurosci.* **13**, 1277. https://doi.org/10.3389/fnins.2019.01277 (2019).
26. Royer, J. et al. Epilepsy and brain network hubs. *Epilepsia* **63**, 537–550. https://doi.org/10.1111/epi.17171 (2022).
27. Rubinov, M. & Bullmore, E. Schizophrenia and abnormal brain network hubs. *Dialogues Clin. Neurosci.* **15**, 339–349. https://doi.org/10.31887/DCNS.2013.15.3/mrubinov (2013).

28. Oldham, S. & Fornito, A. The development of brain network hubs. *Dev. Cogn. Neurosci.* **36**, 100607. https://doi.org/10.1016/j.dcn.2018.12.005 (2019).
29. Hao, S., Yang, C., Li, Z. & Ren, J. Distinguishing patients with Temporal lobe epilepsy from normal controls with the directed graph measures of resting-state fMRI. *Seizure* **96**, 25–33. https://doi.org/10.1016/j.seizure.2022.01.007 (2022).
30. Lin, Y. H. et al. Anatomy and white matter connections of the inferior Temporal gyrus. *World Neurosurg.* **143**, e656–e666. https://doi.org/10.1016/j.wneu.2020.08.058 (2020).
31. Trimmel, K. et al. Left Temporal lobe Language network connectivity in Temporal lobe epilepsy. *Brain* **141**, 2406–2418. https://doi.org/10.1093/brain/awy164 (2018).
32. Liu, Y. et al. Childhood sexual abuse related to brain activity abnormalities in right inferior Temporal gyrus among major depressive disorder. *Neurosci. Lett.* **806**, 137196. https://doi.org/10.1016/j.neulet.2023.137196 (2023).
33. Gliebus, G. P. Memory dysfunction. *Continuum (Minneap Minn)*. **24**, 727–744. https://doi.org/10.1212/con.0000000000000619 (2018).
34. Kim, D. et al. Overconnectivity of the right heschl's and inferior Temporal gyrus correlates with symptom severity in preschoolers with autism spectrum disorder. *Autism Res.* **14**, 2314–2329. https://doi.org/10.1002/aur.2609 (2021).
35. Li, Z., Hu, J., Wang, Z., You, R. & Cao, D. Basal ganglia stroke is associated with altered functional connectivity of the left inferior Temporal gyrus. *J. Neuroimaging*. **32**, 744–751. https://doi.org/10.1111/jon.12978 (2022).
36. Baltaretu, B. R., Dunkley, B. T., Stevens, W. D. & Crawford, J. D. Occipital cortex is modulated by Transsaccadic changes in Spatial frequency: an fMRI study. *Sci. Rep.* **11**, 8611. https://doi.org/10.1038/s41598-021-87506-2 (2021).
37. Wang, J. et al. Combining Gray matter volume in the cuneus and the cuneus-prefrontal connectivity May predict early relapse in abstinent alcohol-dependent patients. *PLoS One*. **13**, e0196860. https://doi.org/10.1371/journal.pone.0196860 (2018).
38. He, X. et al. The morphometry of left cuneus mediating the genetic regulation on working memory. *Hum. Brain Mapp.* **42**, 3470–3480. https://doi.org/10.1002/hbm.25446 (2021).
39. Li, K. et al. Altered spontaneous functional activity of the right precuneus and cuneus in patients with persistent postural-perceptual Dizziness. *Brain Imaging Behav.* **14**, 2176–2186. https://doi.org/10.1007/s11682-019-00168-7 (2020).
40. Palejwala, A. H. et al. Anatomy and white matter connections of the lingual gyrus and cuneus. *World Neurosurg.* **151**, e426–e437. https://doi.org/10.1016/j.wneu.2021.04.050 (2021).
41. Hao, S. et al. A resting-state fMRI study of Temporal lobe epilepsy using multivariate pattern analysis and Granger causality analysis. *J. Neuroimaging*. **32**, 977–990. https://doi.org/10.1111/jon.13012 (2022).
42. Epstein, R. A. & Baker, C. I. Scene perception in the human brain. *Annu. Rev. Vis. Sci.* **5**, 373–397. https://doi.org/10.1146/annurev-vision-091718-014809 (2019).
43. Xu, K., Liu, R., Chen, X., Yang, Y. & Wang, Q. Brain structure variability study in pilots based on VBM. *PLoS One*. **18**, e0276957. https://doi.org/10.1371/journal.pone.0276957 (2023).
44. Li, R. et al. Developmental maturation of the precuneus as a functional core of the default mode network. *J. Cogn. Neurosci.* **31**, 1506–1519. https://doi.org/10.1162/jocn_a_01426 (2019).
45. Flanagin, V. L. et al. The precuneus as a central node in declarative memory retrieval. *Cereb. Cortex*. **33**, 5981–5990. https://doi.org/10.1093/cercor/bhac476 (2023).
46. Dadario, N. B. & Sughrue, M. E. The functional role of the precuneus. *Brain* **146**, 3598–3607. https://doi.org/10.1093/brain/awad181 (2023).
47. Qin, Y. et al. BOLD-fMRI activity informed by network variation of scalp EEG in juvenile myoclonic epilepsy. *Neuroimage Clin.* **22**, 101759. https://doi.org/10.1016/j.nicl.2019.101759 (2019).
48. Husbani, M. A. R. et al. Effective connectivity between precuneus and supramarginal gyrus in healthy subjects and Temporal lobe epileptic patients. *Med. J. Malaysia*. **76**, 360–368 (2021).
49. Guo, Z. et al. Effective connectivity among the hippocampus, amygdala, and Temporal neocortex in epilepsy patients: A cortico-cortical evoked potential study. *Epilepsy Behav.* **115**, 107661. https://doi.org/10.1016/j.yebeh.2020.107661 (2021).
50. Cook, C. J. et al. Effective connectivity within the default mode network in left Temporal lobe epilepsy: findings from the epilepsy connectome project. *Brain Connect.* **9**, 174–183. https://doi.org/10.1089/brain.2018.0600 (2019).
51. Wu, Z. & Buckley, M. J. Prefrontal and medial Temporal lobe cortical contributions to visual Short-Term memory. *J. Cogn. Neurosci.* **35**, 27–43. https://doi.org/10.1162/jocn_a_01937 (2022).
52. Marwood, L., Wise, T., Perkins, A. M. & Cleare, A. J. Meta-analyses of the neural mechanisms and predictors of response to psychotherapy in depression and anxiety. *Neurosci. Biobehavioral Reviews*. **95**, 61–72. https://doi.org/10.1016/j.neubiorev.2018.09.022 (2018).
53. Li, J. et al. Mapping the subcortical connectivity of the human default mode network. *Neuroimage* **245**, 118758. https://doi.org/10.1016/j.neuroimage.2021.118758 (2021).

Author contributions

The contributions are as follows.L.Q : data analysis and writing of the paper draft. J.S: methodology and modifcation of paper draft. M.C: literature research and visualization. Q.Z, Y. H, T. S, L.Q: data acquisition. O.Z: conceptualization, study design, and supervision.All authors reviewed the manuscript.

Declarations

Competing interests

The authors declare no competing interests.

Additional information

Supplementary Information The online version contains supplementary material available at https://doi.org/10.1038/s41598-025-05347-9.

Correspondence and requests for materials should be addressed to J.Z.

Reprints and permissions information is available at www.nature.com/reprints.

Publisher's note Springer Nature remains neutral with regard to jurisdictional claims in published maps and institutional affiliations.